Design of Multiple Constriction Ratio Microfluidic Channels for 3D Insulator based Dielectrophoretic Chips

by

Rand Hidayah

Submitted to the Department of Mechanical Engineering in Partial Fulfillment of the Requirements for the Degree of Bachelor of Science at the Massachusetts Institute of Technology

June 2012

Signature of Author

....

Department of Mechanical Engineering
May 18, 2012

Certified by

....

Cullen R. Buie
Mitsui Career Development Assistant Professor of Mechanical Engineering
Thesis Supervisor

Accepted by

....

John H. Lienhard V
Samuel C. Collins Professor of Mechanical Engineering
Undergraduate Officer

Design of Multiple Constriction Ratio Microfluidic Channels for 3D Insulator based Dielectrophoretic Chips

By

Rand Hidayah

Submitted to the Department of Mechanical Engineering on May 18, 2012 in Partial Fulfillment of the Requirements for the Degree of Bachelors of Science in Mechanical Engineering

ABSTRACT

Insulator based dielectrophoresis (iDEP) is a technique used for sorting microparticles based on their electrical properties which proves to be promising in its development. Using multiple constrictions of area to generate gradients of electric fields allows a device to be made without electrode arrays and at a cheaper cost. The possibility of making devices with multiple constrictions within them is undertaken using micromachining and adhesion methods. The micromachining of multiple constrictions is planned out but further work is needed for optimization. A concept for a commercial device is proposed for low cost fabrication of 3D iDEP devices.

Thesis Supervisor: Cullen R. Buie
Title: Assistant Professor

Acknowledgements

I would first like to thank Professor Cullen Buie for his guidance and support throughout this thesis project. I have learned a lot by the opportunity he has afforded me in working in his lab for the duration of the project.

I would like to thank William Braff, for his patience and guidance around the lab and in the completion of this project. His advice and help was greatly appreciated and his ideas and tools accelerated the work on this thesis immensely.

Substantial thanks go to my family and friends for their personal support and their encouragement throughout my MIT career.

Table of Contents

List of Figures

List of Tables

1. Introduction

1.1 Overview

Insulator based Dielectrophoresis (iDEP) is a technique for sorting microparticles based on their electrical properties which promises to solve many of the problems which arise in more complex sorting systems requiring pumping and microelectrodes [1].

Dielectrophoresis (DEP) is defined as the force due to a non-uniform electric field acting on an induced dipole of a particle suspended in a medium [2]. Recently, insulator based DEP devices have been developed as an alternative to electrode based DEP devices. Insulators in these devices are typically structures which create large field gradients in a uniform electric field along a channel which carries a fluid with suspended particles.

The devices that are of concern in this thesis are microfluidic channels which trap particles suspended in a medium through a varying electric field due to a constriction in the fluid. The trapping occurs due to a balance of DEP force and Stokes drag on the bacteria or particle [1] The physics of which will be discussed later in this thesis.

The devices described and made for the purposes of this thesis are particularly made for multiple trappings of different sized bacteria or particles in one channel. This would be of particular interest for commercial use of the 3D iDEP devices. The devices are prototyped by micro-machining acrylic, but other ways of manufacture are explored in the context of this thesis.

1.2 Dielectrophoresis

DEP is a promising technique used mainly for probing electrical properties of microparticles [2]. It was first observed by Pohl in 1951 [7], it is a phenomenon where a force can be applied to a particle based on the relative polarizabilty of it to the medium surrounding it. This means that a particle in a moving medium faced with a changing electric field can be decelerated or change direction. This is a powerful tool for small microfluidic devices in particular since it removes the need for high voltages, pumps and other mechanical elements which are conventionally used in fluid flow systems for control. Since the channels being made are for bacteria and operate on a micro scale, the DEP force can be a well utilized component of the design of a microfluidic system.

This use for microparticles was established in the nineteen eighties. When DEP was observed for the first time, forces generated were small and did not seem significant for use, it is only with the advent of micro and nanotechnology that the use of DEP has received attention [8].

A spherical homogenous particle with radius a, permittivity ε_m, with Clausius-Mosotti factor κ_{CM}, under a DC voltage generating an electric field E_0 has the following expression for the force on the particle

$$\bar{F} = 2\pi\epsilon_1 a^3 \kappa_{CM} \nabla {E_0}^2 \tag{1.1}$$

Where κ_{CM} is the Clausius-Mossotti factor, which characterizes the relationship between the dielectric constants of two different media, and can be written in terms of the media's ϵ_2 and free spaces' ϵ_1 complex permittivities in this case:

$$\kappa_{CM} = \frac{{\epsilon_2}^* - {\epsilon_1}^*}{{\epsilon_2}^* + 2{\epsilon_1}^*} \tag{1.2}$$

1.3 Application to Microbial Fuel Cells

Microbial fuel cells give a solution for constant, continuous power supply which do not need infrastructure or significant capital investment for their introduction into a power system [6].

Microbial fuel cells work on the same principle as a traditional fuel cell, producing energy from a fuel and oxidant reacting at an anode and cathode and producing a potential difference between them. However a microbial fuel cell does not use electrocatalysts for driving the reaction, it relies on living organisms' ability to oxidize and decompose a natural substrate and transfer electrons to the anode. This method has been optimized in the recent past for power density and small and large scale applications [4].

Improvements in systems design have been and continue to be the cause of the major improvements in microbial fuel cell outputs. However, for the existing strains of bacteria and technologies utilized, the limits are being reached. The main overlap of the microfluidic devices investigated in this thesis lies in the study of the dielectric properties of the bacteria for use in fuels cells. The devices manufactured for this thesis also serve as an experiment to see if multiple constriction ratios can be utilized to characterize different dielectric properties of different particles. This could possibly lead to different uses of the bacteria and a better process for multiple sorting of particles by the same device.

2 Modeling 3D iDEP Devices

Here follows a discussion on the most important parameters in designing the system of microfluidic channels. The Reynolds number of the fluid and the entry length of creeping flow is used to determine the channel length, and the constriction ratios of the channels are used to determine the geometry of the channels.

2.1 Velocities in the Channel and overall Parameters

The three forces acting upon the particles suspended in the medium are electrophoresis, dielectrophoresis and electroosmosis. The respective corresponding expressions for the velocities $\mathbf{v}_{EP}$, $\mathbf{v}_{DEP}$, and $\mathbf{v}_{EO}$ are defined in terms of the respective mobilities, μ_x and the Electric field **E**, which is a function of the total applied voltage V_0 divided by the length of the channel L_{tot}, the viscosity η, the Clausius-Mossotti factor κ_{CM}, the radius r and the permittivity of the medium ϵ:

$$\mathbf{v}_{EP} = -\mu_{EP}\mathbf{E} \tag{2.1}$$

$$\mathbf{v}_{DEP} = -\mu_{DEP}\nabla\mathbf{E}^2 \tag{2.2}$$

$$\mathbf{v}_{\mathrm{EO}} = -\mu_{EO}\mathbf{E} \tag{2.3}$$

The overall parameters used in calculating the relevant behavior of the microfluidic channels are outlined in table 2-1. The dielectrophoretic mobility μ_{DEP} is calculated as a function of κ_{CM}, r, εr, $\varepsilon 0$ and η:

$$\frac{\kappa_{CM}\epsilon_0\epsilon_r r^2}{3\eta} \quad (2.4)$$

TABLE 2-1: Parameters pertaining to the numerical Model of 3D iDEP Microfluidic Channels

Parameter	Value	Units	Meaning
εr	80.1	Ratio	Relative permittivity
ε0	$8.8521 x 10^{-12}$	F/m	Free space permittivity
ρ	10^3	Kg/m^3	Density
η	10^{-3}	Pa s	Viscosity
σm	100	µS/cm	Media conductivity
σp	0	µS/cm	Particle conductivity
κ	-0.5	Ratio	Clausius Mossotti
r	5	µm	Particle radius
μ_{EO}	1.1×10^{-8}	$m^2/(Vs)$	EO mobility
μ_{EP}	7.1×10^{-9}	$m^2/(Vs)$	EP Mobility
μ_{DEP}	5.9×10^{-13}	m^4V^2/s	DEP Mobility
Cp	4200	J/(kgK)	Heat Capacity
k	0.58	W/(mK)	Thermal Conductivity
L	2.813	mm	Channel Length
L_{tot}	10	mm	Total Length
V_0	10 or 50`	Volts	Applied DC Voltage

2.2 Stokes' Flow and Drag on Particles, Trapping Factor

Using the design in the previous section, and the relevant parameters of the setup we find that the Reynold's number, given by the electroosmotic mobility μ_{EO} = 1.1x10^-8 m^2/Vs, with an applied voltage ϕ of 10 -100V. To find the appropriate channel length, the Reynolds number is found using the electroosmotic mobility μ_{EO} and the overall electric field (V_0/L_{tot}) for a velocity, as well as the viscosity, density and hydraulic diameter of the channel.

$$Re = \frac{\mu_{EO}\phi D}{\nu L_{tot}} \tag{2.5}$$

$$= 0.002 - 0.0021$$

Which satisfies the criterion for stokes flow, where Re << 1. The force a spherical particle feels in this case with a thin double layer surrounded by a fluid of dynamic viscosity η is a linear function of the drift velocity and is expressed by:

$$F = 6\eta\pi r v \tag{2.6}$$

The three forces acting on the particles in this system, electroosmosis, electrophoresis and dielectrophoresis govern the velocity at different points in the channel. The trapping occurs when the trapping factor defined as α is greater than 1 [1].

$$\alpha = \frac{-\mu_{DEP}}{\mu_{EO}+-\mu_{EP}}\frac{V_0\chi}{Lw} \tag{2.7}$$

The entry length is calculated by approximation of laminar flow for the channels. It is thus given by [3]:

$$\left(\frac{0.06}{1+0.035Re} + 0.056 * Re\right) D \tag{2.8}$$

Which is calculated as approximately 0.281 mm in length and thus the channels were designed for such parameters.

2.3 Governing Equations and Boundary Conditions

The differential equations that govern the system are concerned with fluid flow, heat transfer and current conservation to characterize the behavior of the system

$$0 = -\nabla \mathrm{p} + \eta \nabla^2 \mathbf{u} \tag{2.9}$$

$$\rho C_p \mathbf{u} \cdot \nabla \mathrm{T} = \mathrm{k} \nabla^2 T + \frac{\mathrm{J} \cdot \mathrm{J}}{\sigma} \tag{2.10}$$

$$0 = \nabla \cdot \mathrm{J} \tag{2.11}$$

The inlet source T_a can be treated as large, the system response time is about 300 seconds, and since the experiment runs for more time than that, it should be sufficient to reach a steady state response with the applied voltage. Axial conduction at the outlet is neglected, and the temperature at the constriction is known to be continuous, which gives the general form of the solution as [5]:

$$\frac{k}{\sigma {V_0}^2}(T1 - Ta) = A_1 e^{\frac{s1x}{L}} + A_2 e^{\frac{s2x}{L}} \tag{2.12}$$

$$\frac{k}{\sigma {V_0}^2}(T1 - Ta) = B_1 e^{\frac{s1x}{L}} + B_2 e^{\frac{s2x}{L}} \tag{2.13}$$

3 Design

3.1 Entrance Length Considerations

The entrance length for fully developed flow was a key parameter to consider in the design of multiple constriction channels, and allow entrance to the next channel with the same velocity profile at the onset of the previous constriction. This was found in section 2, and the length was picked as the minimum length between constrictions.

3.2 Design of 3D iDEP Microfluidic Channels

The design is meant to have three constriction ratios per microfluidic channel. Three reductions of ratios were picked: one which reduces each constriction ratio by half at each stage, one which reduced the constriction ratio by twenty at each stage, and one which reduced the constriction ration by an order of magnitude along the microfluidic channel.

TABLE 3-1: Constriction Ratios and Constriction Dimensions

		Depth (mm)	Width (mm)	χ
Channel 1	Constriction 1	0.05	0.05	100
	Constriction 2	0.05	0.10	50
	Constriction 3	0.05	0.20	25
Channel 2	Constriction 1	0.05	0.05	100
	Constriction 2	0.05	0.0625	80
	Constriction 3	0.05	0.0833	60
Channel 3	Constriction 1	0.05	0.05	100
	Constriction 2	0.1	0.0625	40
	Constriction 3	0.2	0.125	10

3.3 Parameters

There are certain parameters in the design to be adhered to, the material for one, was PMMA (Acrylic) for its optical properties as a clear material, and it's machinability on a mill without much deformation. Since an established code was used for a 2.5 by 5.5 cm acrylic piece, then the channels were designed for those dimensions.

The channel reservoirs would have to by 7 mm apart due to the reservoir diameter being a constraining factor to be glued in. This restricts the amount of channels to be machined on the acrylic plate to 7. This is also a good number of channels to ensure that some will work as the milling tools at this scale are very delicate.

The tools used were the 50 μm, 380 μm and 1.59 mm end mills. Machining time for this operation should be approximately 30 minutes for channels 1 and 2 and 40 minutes for channel 3.

3.4 Schematics

The following engineering drawings are meant to give a sense of the manipulation of dimensions of the various constrictions in the three iDEP channels. These views are similar to the views that would be observed while looking top down from a microscope. The schematics are included to show the dimensions and the varying constriction areas in an engineering context. The manufacturing process would have to take into account the dimensions of the tooling and material which the channels are made of.

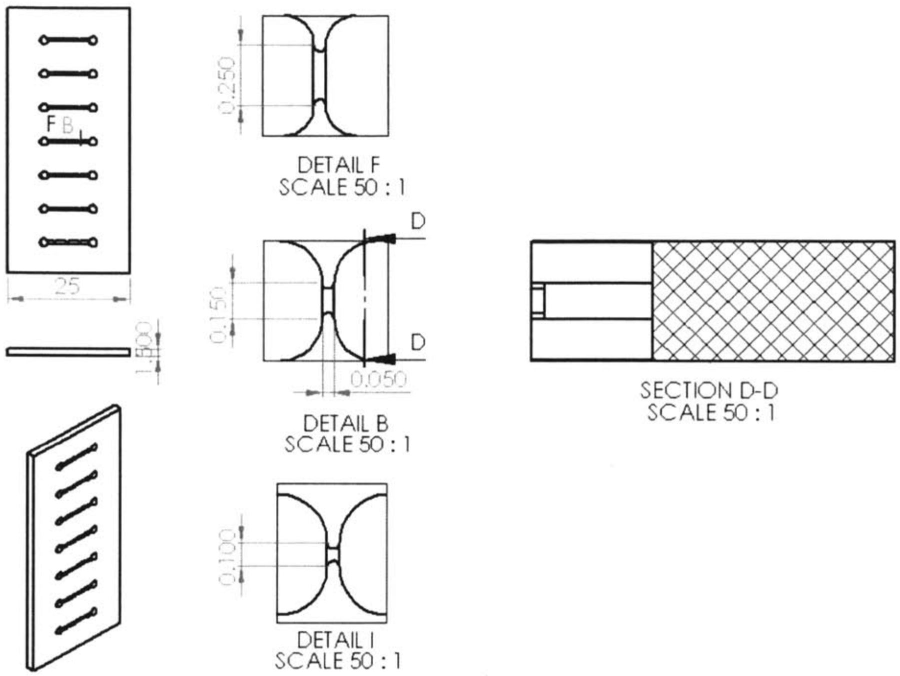

Figure 3-1 Channel 1 with Details on the Dimensions of all Constrictions
All units in millimeters

Note that the constrictions get smaller along the channel, so that the most trapping occurs at the end of the channel.

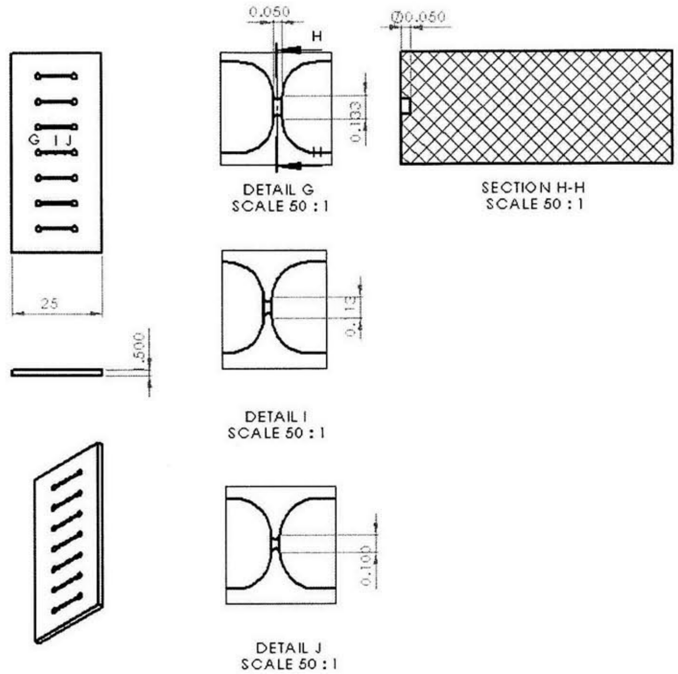

Figure 3-2 Channel 2 with Details on the Dimensions of all Constrictions
All units in millimeters

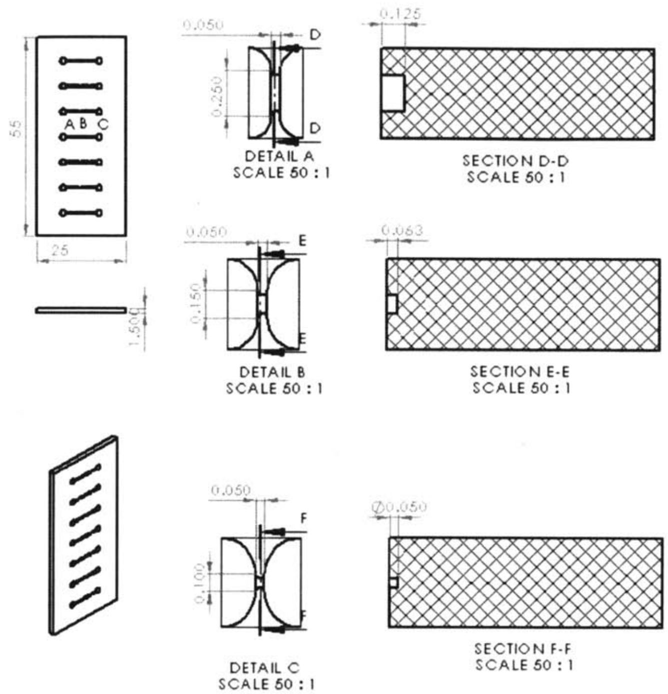

Figure 3-3 Channel 3 with Details on the Dimensions of all Constrictions
All units in millimeters

3.5 3D Model

The iDEP chips are machined to the specs of this Solidworks CAD model, which was used in the generating of G-Code for the micro mill for machining. All the channels have similar geometry to the one shown in Figure 3-4, where the channels are separated by 0.05 mm walls which are machined to form a smaller channel connecting each of the larger channels.

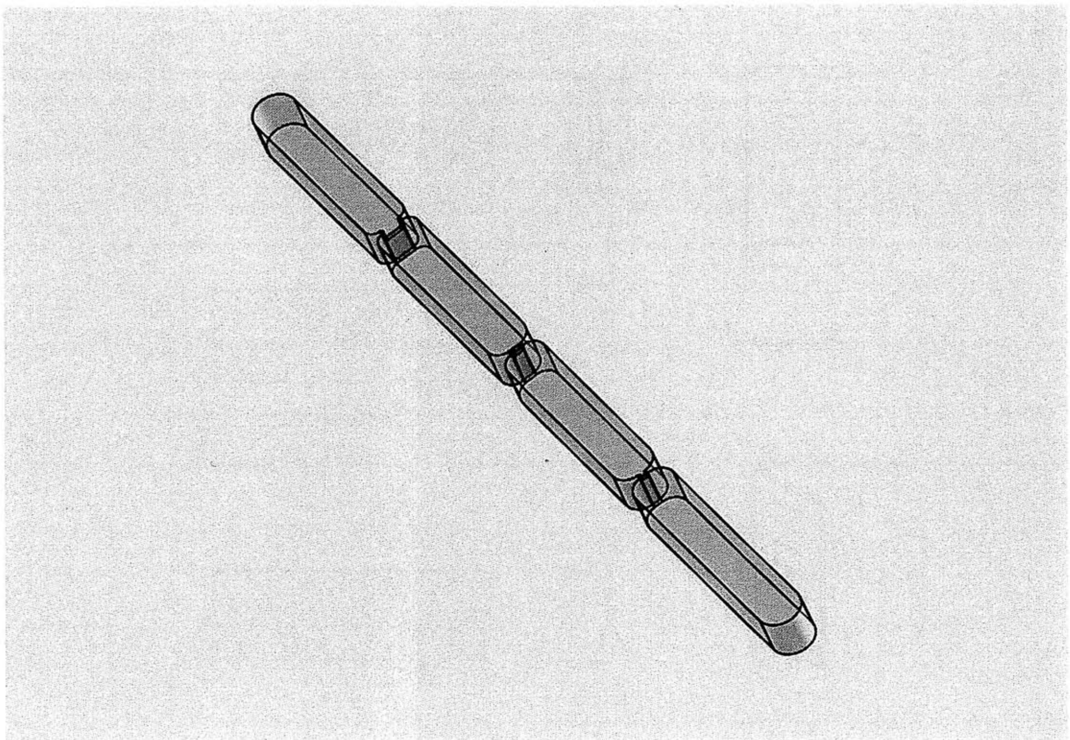

Figure 3-4 3D iDEP Isometric of Channel Geometry

4 Manufacture

The following outlines procedures for manufacture of the 3D iDEP devices using the mill and the oven for curing the adhesives. Cleaning implements and clamps are needed for certain steps to keep the stock clean and constrained as it is prepared to be assembled.

In general the materials needed are PMMA, acetone, methanol, deionized water, tweezers, PMMA Glue, 1.59 mm, 380 micron and 50 micron end mills and solution for running the experiment.

4.1 Procedure

The solution for the experiment was prepared using deionized water, potassium hydroxide and potassium chloride to get the correct conductivity and a neutral pH to run the experiment. The solution was prepared by adding 1 M concentrations of potassium chloride to deionized water to get the correct conductivity of the solution and then adding the 0.1 M concentration potassium hydroxide base to return the pH of the solution to 7.

The acrylic stock is clamped down onto the mill and faced first to establish a starting point for the geometry. Then the g-code should be carried out by the milling program. The steps followed were: mill out the large channels with the 1.5 mm end mill, mill out the reservoirs at a federate of 365 mm/min. Mill out the contours for the constrictions using the 50 micron end mill after a pocket for the needed areas for the constrictions has been machined using the 380 micron end mill. Pocketing the areas with the 380 end mill is essential as the 50 micron end mill can break under such cutting forces. Use a 50 mm/min federate. This process should take slightly longer for Channel 3 as its varying depths mean that the tools need to take more passes to complete the milling job without fracturing.

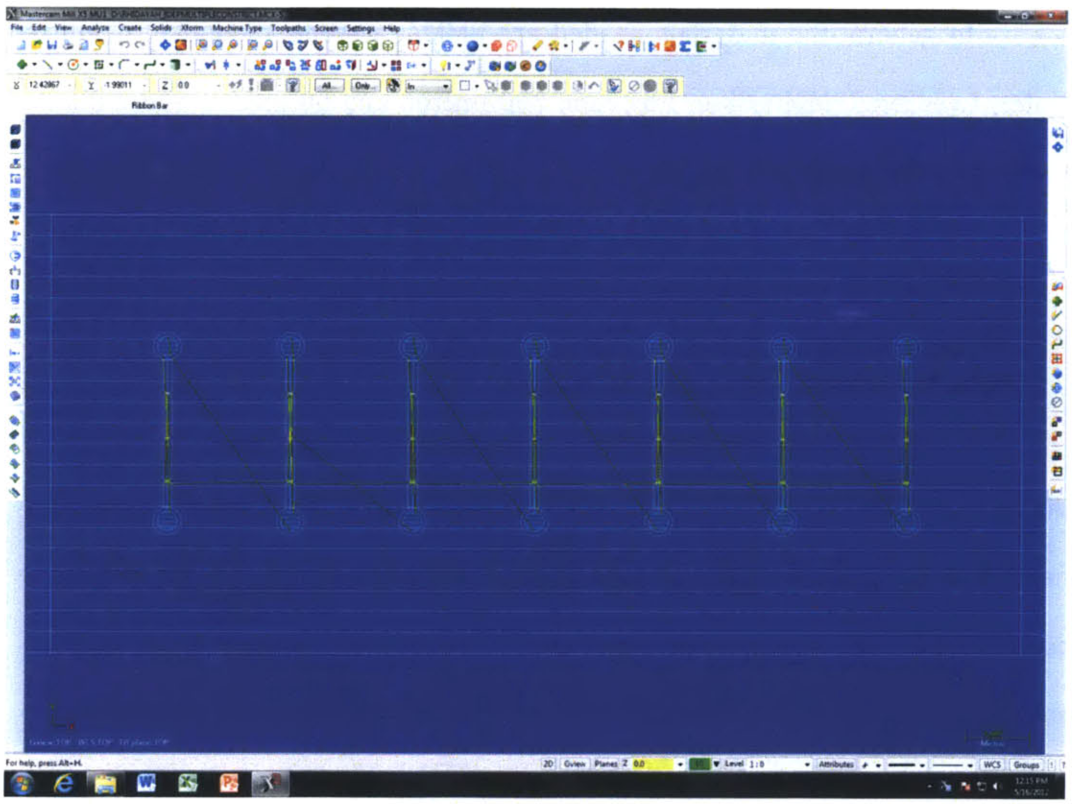

Figure 4-1 MasterCAM Tool Path Image

After the stock has been machined, the part should then be cleaned with methanol, ethanol and deionized water to clear out the channels and checked under a microscope. It is important to take note of checking all the channels for burs and chips which may still be blocking the constrictions. After that has been undertaken, adhesion of the acrylic to another part and curing the assembly is all that is left in the making of the chip. Epoxy and reservoirs may be glued on later for experiments.

A mixture of different sized beads all in florescent dye is injected into the reservoirs and observed under a microscope for validation of the model and the investigation of the trapping factors.

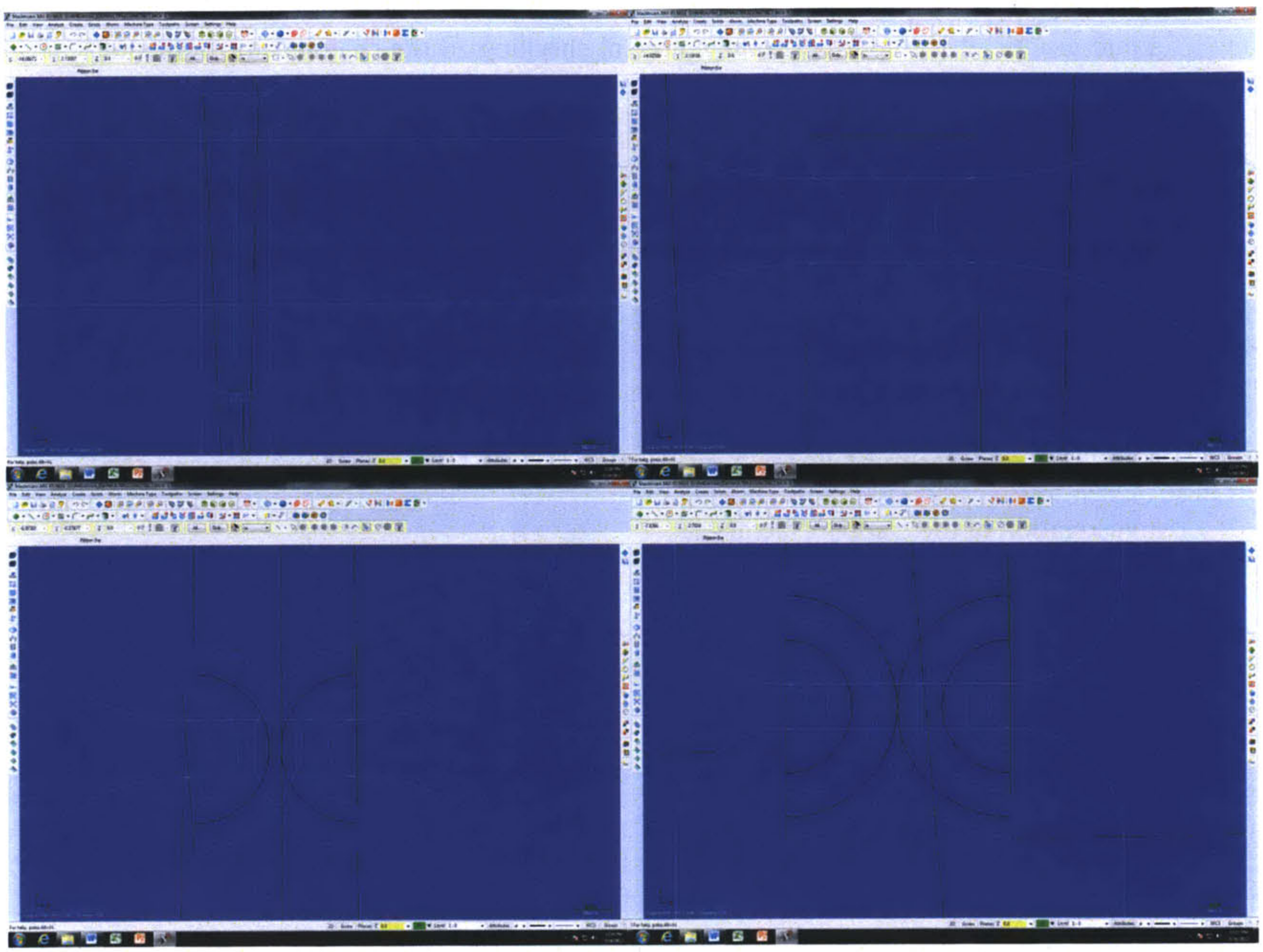

Figure 4-2 Details of the Pocket Milling and Contouring Toolpaths for the MasterCAM Program

4.2 Possible Concept for Commercial Device

The following figures detail a concept for commercializing the device . This would include the assembled chip inserted with conducting elements stopped at the middle of the constriction to be able to take a reading. There may be further analysis required to figure out a how the conducting element will affect the flow of such a system and the optimal geometries and lengths of such chips with multiple constrictions have yet to be optimized. It is projected that the conducting element would be best manufactured by stamping out a conducting metal sheet using a preset stamp. The parts connecting the sensors to the screen could be wires or rigid insulators to help align and give structure to the stamped conducting elements. Some sort of aligning mechanism or test should be undertaken to make sure that the conducting couple is connected to the flow within the constriction, so flexibility within the stamped conducting element is key in making sure that there is compliance for alignment.

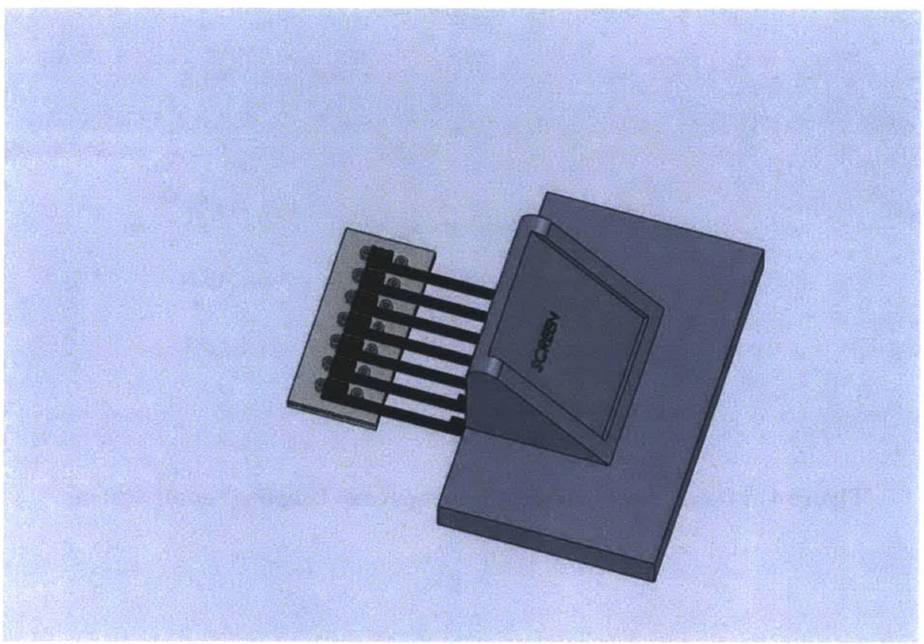

Figure 4-3 Overview of the Design Concept

Figures 4-4 and 4-5 respectively show a detailing of the proposed design concept. The idea behind this is to have a sensor built into the coupling mechanism connected to the screen, and then a monitor would show a reading of a certain variable (Field, Voltage, Flow) to determine a characteristic pertaining to the bacteria or particles in the channel at that point. The dimensions of the assembly are based off the already manufactured chips and a monitor for a pH sensor. The can be modified, as the chip to suit optimal conditions for running such a device. This still remains a concept proposal within the context of the thesis.

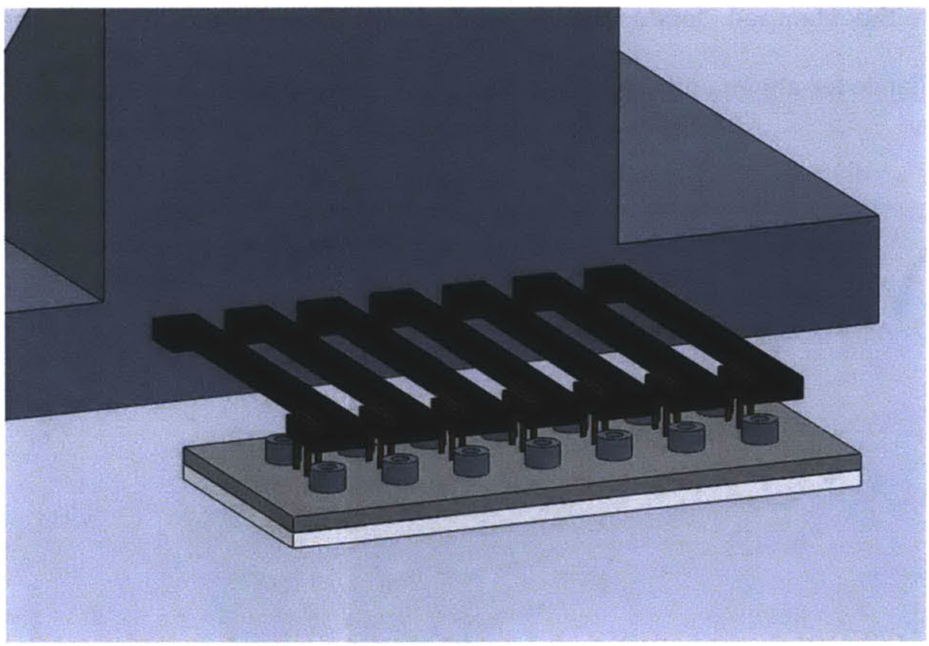

Figure 4 -4 Detailing of Conducting Element and Coupling Sensor System

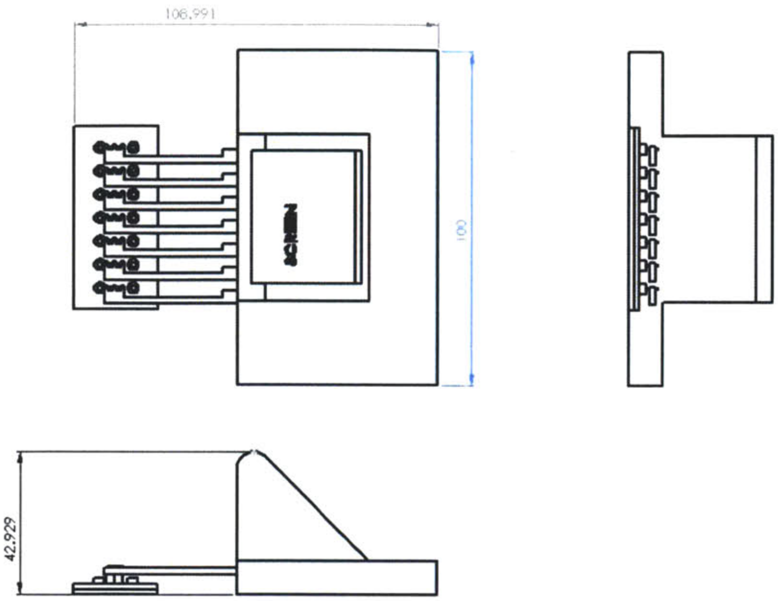

Figure 4 -5 Assembly Schematic with Dimensions in mm

4.3 Manufacturing Results

Due to problems with the Microlution micromill and feed rates in the g-code the channels made were unable to be completed due to the tool breaking and the mill going into error. The channels were not assembled by adhesion due to this manufacturing error. Further investigations into the g-code and its interaction with the mill are necessary in order to understand why the contours and channels did not machine properly. It is possible that a feed rate in the code was set at a non-physical value for the boundaries of the micromill, whereas not forming an error due to the default machine type on MasterCAM.

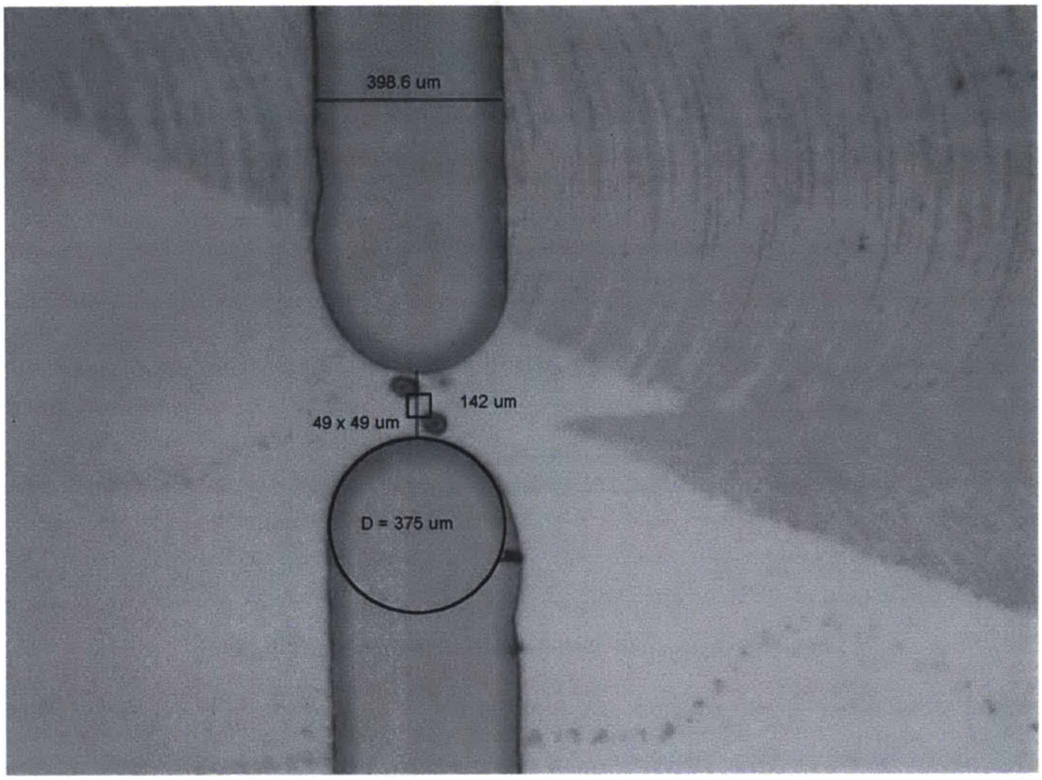

Figure 4-6 Channel dimensions Showing error attempts of the 50 um tool to create contours

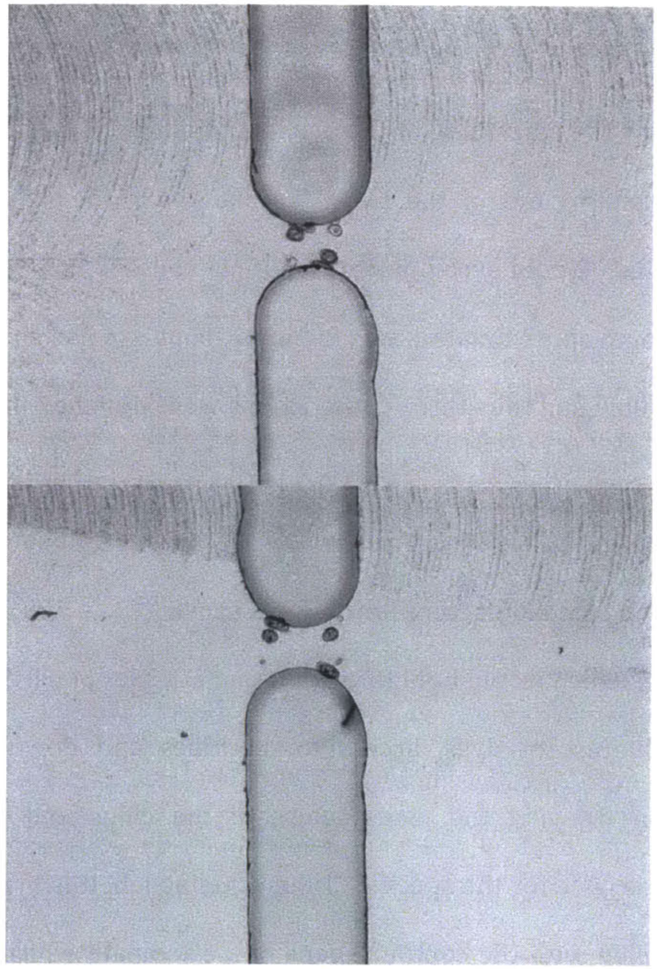

Figure 4-7 Plunge errors at the different channels, showing a widening of the planned constrictions

5 Conclusions

The plan for the machining of the channel took up the largest effort in this thesis was the planning out of the toolpaths and the modeling for an optimal channel length which would accommodate multiple constrictions for the 3D iDEP chip. The entry length approximation was found as about 3 mm of channel to ensure a fully developed flow and thus three constrictions were designed into the 3D iDEP channel.

While a plan for manufacture for multiple constrictions was explored in this work for a channel which would hold three different samples of particle sizes under three different fluorescent dyes, access to machines and downtime played a significant role in delaying the manufacture of the chips and in the loss of troubleshooting the code for the specific CNC machining job. It is hypothesized that the feed rate coupled with the contour shape of the toolpath which machined the constriction. An incorrect plunge rate could have cause the tool to break or insufficient cutting time to fully mill out the constrictions.

Further work should be spent optimizing the manufacturing of the chips before moving onto the concept of a commercial device an sensor. The design concept cannot be worked on without an optimal chip configuration.

Bibliography

[1] W.A. Braff, A. Pignier and C.R. Buie. High Sensitivity three dimensional insulator based dielectrophoresis. *Lab on a Chip* (7):1327-1331 2012.

[2] W.A. Braff, [2011] Manipulation of Bacteria Using Three Dimensional Insulator Based Dielectrophoresis. M. Sc. MIT USA

[3] N. Dombrowski, E. A. Foumeny, S. Ookawara, A. Riza. The Influence of Reynolds Number on the Entry Length and Pressure Drop for Laminar Pipe Flow. *The Canadian Journal of Chemical Engineering* 71, (3): 336-347. 2012.

[4] B.E. Logan Scaling up Microbial Fuel Cells and other bioelectrochemical systems. *Applied Microbiology and Biotechnology*, 85 (6):1665-1671, 2010.

[5] F. Mills. *Heat Transfer*. Prentice Hall, 2nd Edition, 1999

[6] T. Nikam, H.Z. Meymand and M. Nayeripour. A pracitical algorithm for optimal operation management and distribution network including fuel cell power plants. *Renewable Energy* 35, (8): 1696-1714, 2010

[7] H. A. Pohl. The Motion and Precipitation of Suspensoids in Divergent Electric Fields, *J. Appl. Phys.* 22(7), 869–871 (1951).

[8] H.A. Pohl. *Dielectrophoresis*. Cambridge University Press, 1978.

Appendix A: G-Code

```
N1T3M26S1400
N2G0G90G54X-29.249Y12.498
N3Z1.
N4G1Z-.01F0.
N5X28.454F.1
N6G2X29.049Y11.903R.595
N7X28.454Y11.308R.595
N8G1X-28.454
N9G3X-29.049Y10.713R.595
N10X-28.454Y10.117R.595
N11G1X28.454
N12G2X29.049Y9.522R.595
N13X28.454Y8.927R.595
N14G1X-28.454
N15G3X-29.049Y8.332R.595
N16X-28.454Y7.737R.595
N17G1X28.454
N18G2X29.049Y7.142R.595
N19X28.454Y6.547R.595
N20G1X-28.454
N21G3X-29.05Y5.951R.596
N22X-28.454Y5.356R.596
N23G1X28.454
N24G2X29.049Y4.761R.595
N25X28.454Y4.166R.595
N26G1X-28.454
N27G3X-29.049Y3.571R.595
N28X-28.454Y2.976R.595
N29G1X28.454
N30G2X29.049Y2.381R.595
N31X28.454Y1.785R.595
N32G1X-28.454
N33G3X-29.049Y1.19R.595
N34X-28.454Y.595R.595
N35G1X28.454
N36G2X29.049Y0.R.595
N37X28.454Y-.595R.595
N38G1X-28.454
N39G3X-29.049Y-1.19R.595
N40X-28.454Y-1.785R.595
N41G1X28.454
N42G2X29.05Y-2.381R.596
N43X28.454Y-2.976R.596
N44G1X-28.454
N45G3X-29.049Y-3.571R.595
N46X-28.454Y-4.166R.595
N47G1X28.454
N48G2X29.049Y-4.761R.595
N49X28.454Y-5.356R.595
N50G1X-28.454
N51G3X-29.049Y-5.951R.595
N52X-28.454Y-6.547R.595
N53G1X28.454
N54G2X29.049Y-7.142R.595
N55X28.454Y-7.737R.595
N56G1X-28.454
N57G3X-29.049Y-8.332R.595
N58X-28.454Y-8.927R.595
N59G1X28.454
N60G2X29.049Y-9.522R.595
N61X28.454Y-10.117R.595
N62G1X-28.454
N63G3X-29.05Y-10.713R.596
N64X-28.454Y-11.308R.596
N65G1X28.454
N66G2X29.049Y-11.903R.595
N67X28.454Y-12.498R.595
N68G1X-29.249
N69G0Z1.
N70T1M26S1400
N71G0G90G54X-21.01Y-5.544
N72Z1.
N73G1Z-.5F.1
N74X-20.989
N75G3X-20.536Y-5.285R.544
N76G1X-21.464
N77G2X-21.543Y-5.025R.545
N78G1X-20.456
N79X-20.455Y-5.
N80G3X-20.509Y-4.766R.545
N81G1X-21.491
N82G2X-21.228Y-4.506R.544
N83G1X-20.771
N84G0Z1.
N85X-20.825Y-4.474
N86G1Z-.5
N87G2X-20.99Y-4.246R.24
N88G1Y-2.99
N89X-21.01
N90Y-4.246
N91G2X-21.174Y-4.474R.24
N92G3X-21.554Y-5.R.554
N93X-21.Y-5.554R.554
N94X-20.446Y-5.R.554
N95X-20.825Y-4.474R.554
N96G0Z1.
N97X-20.99Y-2.46
N98G1Z-.5
N99Y-.515
N100X-21.01
N101Y-2.46
N102X-20.99
N103G0Z1.
N104Y.015
N105G1Z-.5
N106Y2.035
N107X-21.01
N108Y.015
N109X-20.99
N110G0Z1.
N111X-21.228Y4.506
N112G1Z-.5
N113X-20.771
N114G3X-20.509Y4.766R.544
```

```
N115G1X-21.491
N116G2X-21.544Y5.R.544
N117G1X-21.543Y5.025
N118X-20.456
N119G3X-20.536Y5.284R.545
N120G1X-21.464
N121G2X-21.01Y5.544R.544
N122G1X-20.989
N123G0Z1.
N124X-20.825Y4.474
N125G1Z-.5
N126G3X-20.446Y5.R.554
N127X-21.Y5.554R.554
N128X-21.554Y5.R.554
N129X-21.174Y4.474R.554
N130G2X-21.01Y4.246R.24
N131G1Y2.565
N132X-20.99
N133Y4.246
N134G2X-20.825Y4.474R.24
N135G0Z1.
N136X-14.01Y-5.544
N137G1Z-.5
N138X-13.989
N139G3X-13.536Y-5.285R.544
N140G1X-14.464
N141G2X-14.543Y-5.025R.545
N142G1X-13.456
N143X-13.455Y-5.
N144G3X-13.509Y-4.766R.545
N145G1X-14.491
N146G2X-14.228Y-4.506R.544
N147G1X-13.771
N148G0Z1.
N149X-13.825Y-4.474
N150G1Z-.5
N151G2X-13.99Y-4.246R.24
N152G1Y-2.99
N153X-14.01
N154Y-4.246
N155G2X-14.174Y-4.474R.24
N156G3X-14.554Y-5.R.554
N157X-14.Y-5.554R.554
N158X-13.446Y-5.R.554
N159X-13.825Y-4.474R.554
N160G0Z1.
N161X-14.228Y4.506
N162G1Z-.5
N163X-13.771
N164G3X-13.509Y4.766R.544
N165G1X-14.491
N166G2X-14.544Y5.R.544
N167G1X-14.543Y5.025
N168X-13.456
N169G3X-13.536Y5.284R.545
N170G1X-14.464
N171G2X-14.01Y5.544R.544
N172G1X-13.989
N173G0Z1.
N174X-13.825Y4.474
N175G1Z-.5
N176G3X-13.446Y5.R.554
N177X-14.Y5.554R.554
N178X-14.554Y5.R.554
N179X-14.174Y4.474R.554
N180G2X-14.01Y4.246R.24
N181G1Y2.565
N182X-13.99
N183Y4.246
N184G2X-13.825Y4.474R.24
N185G0Z1.
N186X-13.99Y-.515
N187G1Z-.5
N188X-14.01
N189Y-2.46
N190X-13.99
N191Y-.515
N192G0Z1.
N193Y.015
N194G1Z-.5
N195Y2.035
N196X-14.01
N197Y.015
N198X-13.99
N199G0Z1.
N200X-7.01Y-5.544
N201G1Z-.5
N202X-6.99
N203G3X-6.536Y-5.285R.544
N204G1X-7.464
N205G2X-7.543Y-5.025R.545
N206G1X-6.457
N207X-6.456Y-5.
N208G3X-6.509Y-4.766R.544
N209G1X-7.491
N210G2X-7.229Y-4.506R.544
N211G1X-6.771
N212G0Z1.
N213X-6.825Y-4.474
N214G1Z-.5
N215G2X-6.99Y-4.246R.24
N216G1Y-2.99
N217X-7.01
N218Y-4.246
N219G2X-7.174Y-4.474R.24
N220G3X-7.554Y-5.R.554
N221X-7.Y-5.554R.554
N222X-6.446Y-5.R.554
N223X-6.825Y-4.474R.554
N224G0Z1.
N225X-6.99Y-2.46
N226G1Z-.5
N227Y-.515
N228X-7.01
N229Y-2.46
N230X-6.99
N231G0Z1.
N232Y.015
N233G1Z-.5
N234Y2.035
N235X-7.01
N236Y.015
```

```
N237X-6.99
N238G0Z1.
N239X-7.229Y4.506
N240G1Z-.5
N241X-6.771
N242G3X-6.509Y4.766R.544
N243G1X-7.491
N244G2X-7.544Y5.R.544
N245G1X-7.543Y5.025
N246X-6.457
N247G3X-6.536Y5.284R.544
N248G1X-7.464
N249G2X-7.01Y5.544R.544
N250G1X-6.99
N251G0Z1.
N252X-6.825Y4.474
N253G1Z-.5
N254G3X-6.446Y5.R.554
N255X-7.Y5.554R.554
N256X-7.554Y5.R.554
N257X-7.174Y4.474R.554
N258G2X-7.01Y4.246R.24
N259G1Y2.565
N260X-6.99
N261Y4.246
N262G2X-6.825Y4.474R.24
N263G0Z1.
N264X-.01Y-5.544
N265G1Z-.5
N266X.01
N267G3X.464Y-5.285R.544
N268G1X-.464
N269G2X-.543Y-5.025R.545
N270G1X.543
N271X.544Y-5.
N272G3X.491Y-4.766R.544
N273G1X-.491
N274G2X-.229Y-4.506R.544
N275G1X.229
N276G0Z1.
N277X.174Y-4.474
N278G1Z-.5
N279G2X.01Y-4.246R.24
N280G1Y-2.99
N281X-.01
N282Y-4.246
N283G2X-.174Y-4.474R.24
N284G3X-.554Y-5.R.554
N285X0.Y-5.554R.554
N286X.554Y-5.R.554
N287X.174Y-4.474R.554
N288G0Z1.
N289X.01Y-2.46
N290G1Z-.5
N291Y-.515
N292X-.01
N293Y-2.46
N294X.01
N295G0Z1.
N296Y.015
N297G1Z-.5
N298Y2.035
N299X-.01
N300Y.015
N301X.01
N302G0Z1.
N303X-.229Y4.506
N304G1Z-.5
N305X.229
N306G3X.491Y4.766R.544
N307G1X-.491
N308G2X-.544Y5.R.544
N309G1X-.543Y5.025
N310X.543
N311G3X.464Y5.284R.544
N312G1X-.464
N313G2X-.01Y5.544R.544
N314G1X.01
N315G0Z1.
N316X.174Y4.474
N317G1Z-.5
N318G3X.554Y5.R.554
N319X0.Y5.554R.554
N320X-.554Y5.R.554
N321X-.174Y4.474R.554
N322G2X-.01Y4.246R.24
N323G1Y2.565
N324X.01
N325Y4.246
N326G2X.174Y4.474R.24
N327G0Z1.
N328X6.99Y-5.544
N329G1Z-.5
N330X7.01
N331G3X7.464Y-5.285R.544
N332G1X6.536
N333G2X6.457Y-5.025R.545
N334G1X7.543
N335X7.544Y-5.
N336G3X7.491Y-4.766R.544
N337G1X6.509
N338G2X6.771Y-4.506R.544
N339G1X7.229
N340G0Z1.
N341X7.174Y-4.474
N342G1Z-.5
N343G2X7.01Y-4.246R.24
N344G1Y-2.99
N345X6.99
N346Y-4.246
N347G2X6.826Y-4.474R.24
N348G3X6.446Y-5.R.554
N349X7.Y-5.554R.554
N350X7.554Y-5.R.554
N351X7.174Y-4.474R.554
N352G0Z1.
N353X7.01Y-2.46
N354G1Z-.5
N355Y-.515
N356X6.99
N357Y-2.46
N358X7.01
```

```
N359G0Z1.
N360Y.015
N361G1Z-.5
N362Y2.035
N363X6.99
N364Y.015
N365X7.01
N366G0Z1.
N367X6.771Y4.506
N368G1Z-.5
N369X7.229
N370G3X7.491Y4.766R.544
N371G1X6.509
N372G2X6.456Y5.R.544
N373G1X6.457Y5.025
N374X7.543
N375G3X7.464Y5.284R.544
N376G1X6.536
N377G2X6.99Y5.544R.544
N378G1X7.01
N379G0Z1.
N380X7.174Y4.474
N381G1Z-.5
N382G3X7.554Y5.R.554
N383X7.Y5.554R.554
N384X6.446Y5.R.554
N385X6.826Y4.474R.554
N386G2X6.99Y4.246R.24
N387G1Y2.565
N388X7.01
N389Y4.246
N390G2X7.174Y4.474R.24
N391G0Z1.
N392X13.99Y-5.544
N393G1Z-.5
N394X14.01
N395G3X14.464Y-5.285R.544
N396G1X13.536
N397G2X13.457Y-5.025R.545
N398G1X14.543
N399X14.544Y-5.
N400G3X14.491Y-4.766R.544
N401G1X13.509
N402G2X13.771Y-4.506R.544
N403G1X14.229
N404G0Z1.
N405X14.174Y-4.474
N406G1Z-.5
N407G2X14.01Y-4.246R.24
N408G1Y-2.99
N409X13.99
N410Y-4.246
N411G2X13.826Y-4.474R.24
N412G3X13.446Y-5.R.554
N413X14.Y-5.554R.554
N414X14.554Y-5.R.554
N415X14.174Y-4.474R.554
N416G0Z1.
N417X14.01Y-2.46
N418G1Z-.5
N419Y-.515
N420X13.99
N421Y-2.46
N422X14.01
N423G0Z1.
N424Y.015
N425G1Z-.5
N426Y2.035
N427X13.99
N428Y.015
N429X14.01
N430G0Z1.
N431X13.771Y4.506
N432G1Z-.5
N433X14.229
N434G3X14.491Y4.766R.544
N435G1X13.509
N436G2X13.456Y5.R.544
N437G1X13.457Y5.025
N438X14.543
N439G3X14.464Y5.284R.544
N440G1X13.536
N441G2X13.99Y5.544R.544
N442G1X14.01
N443G0Z1.
N444X14.174Y4.474
N445G1Z-.5
N446G3X14.554Y5.R.554
N447X14.Y5.554R.554
N448X13.446Y5.R.554
N449X13.826Y4.474R.554
N450G2X13.99Y4.246R.24
N451G1Y2.565
N452X14.01
N453Y4.246
N454G2X14.174Y4.474R.24
N455G0Z1.
N456X20.99Y-5.544
N457G1Z-.5
N458X21.01
N459G3X21.464Y-5.285R.544
N460G1X20.536
N461G2X20.457Y-5.025R.545
N462G1X21.543
N463X21.544Y-5.
N464G3X21.491Y-4.766R.544
N465G1X20.509
N466G2X20.772Y-4.506R.544
N467G1X21.229
N468G0Z1.
N469X21.174Y-4.474
N470G1Z-.5
N471G2X21.01Y-4.246R.24
N472G1Y-2.99
N473X20.99
N474Y-4.246
N475G2X20.826Y-4.474R.24
N476G3X20.446Y-5.R.554
N477X21.Y-5.554R.554
N478X21.554Y-5.R.554
N479X21.174Y-4.474R.554
N480G0Z1.
```

```
N481X21.01Y-2.46
N482G1Z-.5
N483Y-.515
N484X20.99
N485Y-2.46
N486X21.01
N487G0Z1.
N488Y.015
N489G1Z-.5
N490Y2.035
N491X20.99
N492Y.015
N493X21.01
N494G0Z1.
N495X20.772Y4.506
N496G1Z-.5
N497X21.229
N498G3X21.491Y4.766R.544
N499G1X20.509
N500G2X20.456Y5.R.544
N501G1X20.457Y5.025
N502X21.543
N503G3X21.464Y5.284R.544
N504G1X20.536
N505G2X20.99Y5.544R.544
N506G1X21.01
N507G0Z1.
N508X21.174Y4.474
N509G1Z-.5
N510G3X21.554Y5.R.554
N511X21.Y5.554R.554
N512X20.446Y5.R.554
N513X20.826Y4.474R.554
N514G2X20.99Y4.246R.24
N515G1Y2.565
N516X21.01
N517Y4.246
N518G2X21.174Y4.474R.24
N519G0Z1.
N520T2M26S1400
N521G0G90G54X-21.125Y-2.775
N522Z1.
N523G1Z-.05F0.
N524G3X-21.075Y-2.725R.05
N525X-21.125Y-2.675R.05
N526G0Z1.
N527Y-2.825
N528G1Z-.05
N529G3X-21.025Y-2.725R.1
N530X-21.125Y-2.625R.1
N531G0Z1.
N532Y-2.875
N533G1Z-.05
N534G3X-20.975Y-2.725R.15
N535X-21.125Y-2.575R.15
N536G0Z1.
N537X-21.075Y-.3
N538G1Z-.05
N539G3X-21.025Y-.25R.05
N540X-21.075Y-.2R.05
N541G0Z1.
N542X-21.065Y-.34
N543G1Z-.05
N544G3X-20.975Y-.25R.09
N545X-21.065Y-.16R.09
N546G0Z1.
N547X-21.05Y2.25
N548G1Z-.05
N549G3X-21.Y2.3R.05
N550X-21.05Y2.35R.05
N551G0Z1.
N552X-20.95
N553G1Z-.05
N554G3X-21.Y2.3R.05
N555X-20.95Y2.25R.05
N556G0Z1.
N557X-20.925Y-.2
N558G1Z-.05
N559G3X-20.975Y-.25R.05
N560X-20.925Y-.3R.05
N561G0Z1.
N562Y-.16
N563G1Z-.05
N564G3X-21.015Y-.25R.09
N565X-20.925Y-.34R.09
N566G0Z1.
N567X-20.875Y-2.675
N568G1Z-.05
N569G3X-20.925Y-2.725R.05
N570X-20.875Y-2.775R.05
N571G0Z1.
N572Y-2.625
N573G1Z-.05
N574G3X-20.975Y-2.725R.1
N575X-20.875Y-2.825R.1
N576G0Z1.
N577Y-2.575
N578G1Z-.05
N579G3X-21.025Y-2.725R.15
N580X-20.875Y-2.875R.15
N581G0Z1.
N582X-14.125Y-2.675
N583G1Z-.05
N584G2X-14.075Y-2.725R.05
N585X-14.125Y-2.775R.05
N586G0Z1.
N587Y-2.825
N588G1Z-.05
N589G3X-14.025Y-2.725R.1
N590X-14.125Y-2.625R.1
N591G0Z1.
N592Y-2.875
N593G1Z-.05
N594G3X-13.975Y-2.725R.15
N595X-14.125Y-2.575R.15
N596G0Z1.
N597X-14.075Y-.3
N598G1Z-.05
N599G3X-14.025Y-.25R.05
N600X-14.075Y-.2R.05
N601G0Z1.
N602X-14.065Y-.34
```

```
N603G1Z-.05
N604G3X-13.975Y-.25R.09
N605X-14.065Y-.16R.09
N606G0Z1.
N607X-14.05Y2.25
N608G1Z-.05
N609G3X-14.Y2.3R.05
N610X-14.05Y2.35R.05
N611G0Z1.
N612X-13.95
N613G1Z-.05
N614G3X-14.Y2.3R.05
N615X-13.95Y2.25R.05
N616G0Z1.
N617X-13.925Y-.2
N618G1Z-.05
N619G3X-13.975Y-.25R.05
N620X-13.925Y-.3R.05
N621G0Z1.
N622Y-.16
N623G1Z-.05
N624G3X-14.015Y-.25R.09
N625X-13.925Y-.34R.09
N626G0Z1.
N627X-13.875Y-2.675
N628G1Z-.05
N629G3X-13.925Y-2.725R.05
N630X-13.875Y-2.775R.05
N631G0Z1.
N632Y-2.625
N633G1Z-.05
N634G3X-13.975Y-2.725R.1
N635X-13.875Y-2.825R.1
N636G0Z1.
N637Y-2.575
N638G1Z-.05
N639G3X-14.025Y-2.725R.15
N640X-13.875Y-2.875R.15
N641G0Z1.
N642X-7.125Y-2.775
N643G1Z-.05
N644G3X-7.075Y-2.725R.05
N645X-7.125Y-2.675R.05
N646G0Z1.
N647Y-2.825
N648G1Z-.05
N649G3X-7.025Y-2.725R.1
N650X-7.125Y-2.625R.1
N651G0Z1.
N652Y-2.875
N653G1Z-.05
N654G3X-6.975Y-2.725R.15
N655X-7.125Y-2.575R.15
N656G0Z1.
N657X-7.075Y-.3
N658G1Z-.05
N659G3X-7.025Y-.25R.05
N660X-7.075Y-.2R.05
N661G0Z1.
N662X-7.065Y-.34
N663G1Z-.05
N664G3X-6.975Y-.25R.09
N665X-7.065Y-.16R.09
N666G0Z1.
N667X-7.05Y2.25
N668G1Z-.05
N669G3X-7.Y2.3R.05
N670X-7.05Y2.35R.05
N671G0Z1.
N672X-6.95
N673G1Z-.05
N674G3X-7.Y2.3R.05
N675X-6.95Y2.25R.05
N676G0Z1.
N677X-6.925Y-.2
N678G1Z-.05
N679G3X-6.975Y-.25R.05
N680X-6.925Y-.3R.05
N681G0Z1.
N682Y-.16
N683G1Z-.05
N684G3X-7.015Y-.25R.09
N685X-6.925Y-.34R.09
N686G0Z1.
N687X-6.875Y-2.675
N688G1Z-.05
N689G3X-6.925Y-2.725R.05
N690X-6.875Y-2.775R.05
N691G0Z1.
N692Y-2.625
N693G1Z-.05
N694G3X-6.975Y-2.725R.1
N695X-6.875Y-2.825R.1
N696G0Z1.
N697Y-2.575
N698G1Z-.05
N699G3X-7.025Y-2.725R.15
N700X-6.875Y-2.875R.15
N701G0Z1.
N702X-.125Y-2.775
N703G1Z-.05
N704G3X-.075Y-2.725R.05
N705X-.125Y-2.675R.05
N706G0Z1.
N707Y-2.825
N708G1Z-.05
N709G3X-.025Y-2.725R.1
N710X-.125Y-2.625R.1
N711G0Z1.
N712Y-2.875
N713G1Z-.05
N714G3X.025Y-2.725R.15
N715X-.125Y-2.575R.15
N716G0Z1.
N717X-.075Y-.3
N718G1Z-.05
N719G3X-.025Y-.25R.05
N720X-.075Y-.2R.05
N721G0Z1.
N722X-.065Y-.34
N723G1Z-.05
N724G3X.025Y-.25R.09
```

```
N725X-.065Y-.16R.09
N726G0Z1.
N727X-.05Y2.25
N728G1Z-.05
N729G3X0.Y2.3R.05
N730X-.05Y2.35R.05
N731G0Z1.
N732X.05
N733G1Z-.05
N734G3X0.Y2.3R.05
N735X.05Y2.25R.05
N736G0Z1.
N737X.075Y-.2
N738G1Z-.05
N739G3X.025Y-.25R.05
N740X.075Y-.3R.05
N741G0Z1.
N742Y-.16
N743G1Z-.05
N744G3X-.015Y-.25R.09
N745X.075Y-.34R.09
N746G0Z1.
N747X.125Y-2.675
N748G1Z-.05
N749G3X.075Y-2.725R.05
N750X.125Y-2.775R.05
N751G0Z1.
N752Y-2.625
N753G1Z-.05
N754G3X.025Y-2.725R.1
N755X.125Y-2.825R.1
N756G0Z1.
N757Y-2.575
N758G1Z-.05
N759G3X-.025Y-2.725R.15
N760X.125Y-2.875R.15
N761G0Z1.
N762X6.875Y-2.775
N763G1Z-.05
N764G3X6.925Y-2.725R.05
N765X6.875Y-2.675R.05
N766G0Z1.
N767Y-2.825
N768G1Z-.05
N769G3X6.975Y-2.725R.1
N770X6.875Y-2.625R.1
N771G0Z1.
N772Y-2.875
N773G1Z-.05
N774G3X7.025Y-2.725R.15
N775X6.875Y-2.575R.15
N776G0Z1.
N777X6.925Y-.3
N778G1Z-.05
N779G3X6.975Y-.25R.05
N780X6.925Y-.2R.05
N781G0Z1.
N782X6.935Y-.34
N783G1Z-.05
N784G3X7.025Y-.25R.09
N785X6.935Y-.16R.09
N786G0Z1.
N787X6.95Y2.25
N788G1Z-.05
N789G3X7.Y2.3R.05
N790X6.95Y2.35R.05
N791G0Z1.
N792X7.05
N793G1Z-.05
N794G3X7.Y2.3R.05
N795X7.05Y2.25R.05
N796G0Z1.
N797X7.075Y-.2
N798G1Z-.05
N799G3X7.025Y-.25R.05
N800X7.075Y-.3R.05
N801G0Z1.
N802Y-.16
N803G1Z-.05
N804G3X6.985Y-.25R.09
N805X7.075Y-.34R.09
N806G0Z1.
N807X7.125Y-2.675
N808G1Z-.05
N809G3X7.075Y-2.725R.05
N810X7.125Y-2.775R.05
N811G0Z1.
N812Y-2.625
N813G1Z-.05
N814G3X7.025Y-2.725R.1
N815X7.125Y-2.825R.1
N816G0Z1.
N817Y-2.575
N818G1Z-.05
N819G3X6.975Y-2.725R.15
N820X7.125Y-2.875R.15
N821G0Z1.
N822X13.875Y-2.775
N823G1Z-.05
N824G3X13.925Y-2.725R.05
N825X13.875Y-2.675R.05
N826G0Z1.
N827Y-2.825
N828G1Z-.05
N829G3X13.975Y-2.725R.1
N830X13.875Y-2.625R.1
N831G0Z1.
N832Y-2.875
N833G1Z-.05
N834G3X14.025Y-2.725R.15
N835X13.875Y-2.575R.15
N836G0Z1.
N837X13.925Y-.3
N838G1Z-.05
N839G3X13.975Y-.25R.05
N840X13.925Y-.2R.05
N841G0Z1.
N842X13.935Y-.34
N843G1Z-.05
N844G3X14.025Y-.25R.09
N845X13.935Y-.16R.09
N846G0Z1.
```

```
N847X13.95Y2.25
N848G1Z-.05
N849G3X14.Y2.3R.05
N850X13.95Y2.35R.05
N851G0Z1.
N852X14.05
N853G1Z-.05
N854G3X14.Y2.3R.05
N855X14.05Y2.25R.05
N856G0Z1.
N857X14.075Y-.2
N858G1Z-.05
N859G3X14.025Y-.25R.05
N860X14.075Y-.3R.05
N861G0Z1.
N862Y-.16
N863G1Z-.05
N864G3X13.985Y-.25R.09
N865X14.075Y-.34R.09
N866G0Z1.
N867X14.125Y-2.675
N868G1Z-.05
N869G3X14.075Y-2.725R.05
N870X14.125Y-2.775R.05
N871G0Z1.
N872Y-2.625
N873G1Z-.05
N874G3X14.025Y-2.725R.1
N875X14.125Y-2.825R.1
N876G0Z1.
N877Y-2.575
N878G1Z-.05
N879G3X13.975Y-2.725R.15
N880X14.125Y-2.875R.15
N881G0Z1.
N882X20.875Y-2.775
N883G1Z-.05
N884G3X20.925Y-2.725R.05
N885X20.875Y-2.675R.05
N886G0Z1.
N887Y-2.825
N888G1Z-.05
N889G3X20.975Y-2.725R.1
N890X20.875Y-2.625R.1
N891G0Z1.
N892Y-2.875
N893G1Z-.05
N894G3X21.025Y-2.725R.15
N895X20.875Y-2.575R.15
N896G0Z1.
N897X20.925Y-.3
N898G1Z-.05
N899G3X20.975Y-.25R.05
N900X20.925Y-.2R.05
N901G0Z1.
N902X20.935Y-.34
N903G1Z-.05
N904G3X21.025Y-.25R.09
N905X20.935Y-.16R.09
N906G0Z1.
N907X20.95Y2.25
N908G1Z-.05
N909G3X21.Y2.3R.05
N910X20.95Y2.35R.05
N911G0Z1.
N912X21.05
N913G1Z-.05
N914G3X21.Y2.3R.05
N915X21.05Y2.25R.05
N916G0Z1.
N917X21.075Y-.2
N918G1Z-.05
N919G3X21.025Y-.25R.05
N920X21.075Y-.3R.05
N921G0Z1.
N922Y-.16
N923G1Z-.05
N924G3X20.985Y-.25R.09
N925X21.075Y-.34R.09
N926G0Z1.
N927X21.125Y-2.675
N928G1Z-.05
N929G3X21.075Y-2.725R.05
N930X21.125Y-2.775R.05
N931G0Z1.
N932Y-2.625
N933G1Z-.05
N934G3X21.025Y-2.725R.1
N935X21.125Y-2.825R.1
N936G0Z1.
N937Y-2.575
N938G1Z-.05
N939G3X20.975Y-2.725R.15
N940X21.125Y-2.875R.15
N941G0Z1.
N942M26
N943M30
```